Chemical Science

ROYAL SOCIETY OF CHEMISTRY

EDGE ARTICLE

View Article Online
View Journal | View Issue

Cite this: *Chem. Sci.*, 2025, **16**, 7864

All publication charges for this article have been paid for by the Royal Society of Chemistry

Unconventional pathway for the gas-phase formation of 14π-PAHs *via* self-reaction of the resonantly stabilized radical fulvenallenyl ($C_7H_5^{\bullet}$)†

Wang Li,‡[a] Mengqi Wu,‡[b] Changyang Wang,[a] Jiabin Huang,[b] Jiuzhong Yang,[a] Minggao Xu,[a] Feng Zhang,*[bc] Tao Yang*[def] and Long Zhao*[gh]

Resonantly stabilized free radicals (RSFRs) are contemplated to be the reactive intermediates in molecular mass-growth processes leading to polycyclic aromatic hydrocarbons (PAHs), which are prevalent in deep space and on Earth. The self-reaction routes of two RSFRs have been recognized as fundamental but more-efficient pathways to form fused benzenoid rings. The present experiment, which exploits a chemical microreactor in combination with an isomer-selective identification technique through fragment-free photoionization utilizing a tunable vacuum ultraviolet (VUV) light in tandem with the detection of the ionized molecules by a high-resolution reflection time-of-flight mass spectrometer (Re-TOF-MS), provides compelling evidence for the formation of phenanthrene and a minor amount of anthracene in the presence of fulvenallenyl ($C_7H_5^{\bullet}$). Further theoretical calculations of the potential energy surfaces of $C_{14}H_{10}$ and $C_{14}H_{11}$ reveal that phenanthrene and anthracene can be efficiently produced *via* a hydrogen-assisted multi-step mechanism [$C_7H_5^{\bullet}$ + $C_7H_5^{\bullet}$ → i3, i3 = (3,4-di(cyclopenta-2,4-dien-1-ylidene)cyclobut-1-ene); i3 + H → phenanthrene + H/anthracene + H or i3 + H → i8 + H → phenanthrene + H/anthracene + H, i8 = (1-(cyclopenta-2,4-dien-1-ylidene)indene)] at low pressures, rather than through the one-step recombination–isomerization of fulvenallenyl radicals. This study provides a novel growth mechanism for tricyclic PAHs, especially in hydrogen-rich environments such as combustion and interstellar environments, which advances the knowledge of PAH propagation and even the formation mechanisms of carbonaceous nanoparticles in our universe.

Received 8th January 2025
Accepted 6th March 2025

DOI: 10.1039/d5sc00160a

rsc.li/chemical-science

Introduction

Polycyclic aromatic hydrocarbons (PAHs), which are composed of fused benzenoid rings, are ubiquitous in combustion environments,[1,2] the hydrocarbon-rich atmospheres of planets and satellites, like that of Titan,[3,4] planetary nebulae such as TC 1,[5,6] in the interstellar medium (ISM) in forms including small carbon clusters, fullerenes, and carbonaceous nanoparticles,[7,8] and in the circumstellar envelopes of carbon-rich Asymptotic Giant Branch (AGB) stars,[9,10] such as IRC+10216.[11,12] They represent up to 20% of the total carbon content in our universe.[13] Additionally, PAHs have been in the spotlight as potential candidates to untangle the molecules of the unidentified infrared (UIR) emission bands[14] and the diffuse interstellar bands (DIBs).[15,16] PAHs are also closely relevant to the abiotic synthesis of biorelevant molecules, which are essential to the earliest forms of life.[17,18] Notably, PAHs are recognized as a crucial 'bridge' linking resonantly stabilized free radicals (RSFRs), which have a critical impact on the final formation and the abundance of nanoparticles,[19] with carbonaceous nanoparticles in combustion and extraterrestrial environments.

Much attention has been paid to the mechanisms of PAH formation *via* radical–molecule reactions,[4] while there is a paucity of research into RSFR recombination processes. Radical–radical chain reactions, especially for RSFR recombination, have been proven to be an effective route for rapid hydrocarbon growth in both low- and high-temperature

[a]*National Synchrotron Radiation Laboratory, University of Science and Technology of China, Hefei, Anhui 230029, China*

[b]*Hefei National Research Center for Physical Sciences at the Microscale, University of Science and Technology of China, Hefei, Anhui 230026, China. E-mail: feng2011@ustc.edu.cn*

[c]*Hefei National Laboratory, University of Science and Technology of China, Hefei, Anhui 230088, China*

[d]*State Key Laboratory of Precision Spectroscopy, East China Normal University, Shanghai 200062, China. E-mail: tyang@lps.ecnu.edu.cn*

[e]*Xinjiang Astronomical Observatory, Chinese Academy of Sciences, 150 Science 1-Street, Urumqi, Xinjiang 830011, China*

[f]*Collaborative Innovation Center of Extreme Optics, Shanxi University, Taiyuan, Shanxi 030006, China*

[g]*School of Nuclear Science and Technology, University of Science and Technology of China, Hefei, Anhui 230027, China. E-mail: zhaolong@ustc.edu.cn*

[h]*Deep Space Exploration Laboratory, University of Science and Technology of China, Hefei, Anhui 230026, China*

† Electronic supplementary information (ESI) available. See DOI: https://doi.org/10.1039/d5sc00160a

‡ Both authors contributed equally to this paper.

environments.[20,21] Only a few RSFR recombination systems (Scheme 1), including propargyl($C_3H_3^{\bullet}$)–propargyl recombination to generate benzene (C_6H_6),[22] cyclopentadienyl ($C_5H_5^{\bullet}$)–cyclopentadienyl recombination to generate naphthalene ($C_{10}H_8$),[23] benzyl ($C_7H_7^{\bullet}$)–benzyl recombination to generate phenanthrene/anthracene ($C_{14}H_{10}$), and indenyl ($C_9H_7^{\bullet}$)–indenyl recombination to generate chrysene/benzo[*c*]phenanthrene/benz[*a*]anthracene ($C_{18}H_{12}$),[24] have been explored theoretically and/or directly validated in molecular beam experiments. Inspired by the discovery of cyclic species in the ISM, such as C_5H_5CN (ref. 25) and $C_5H_5C_2H$,[26] PAH formation mechanisms involving RSFRs with five-membered carbon rings are now coming into sight,[23,27] reminding researchers of the possible absence of some vital PAH formation pathways in the current chemical networks.

Fulvenallenyl ($C_7H_5^{\bullet}$) (Scheme 2b), which consists of a five-membered carbon ring and an allenic moiety, has been calculated to be a resonance-stabilized radical[28] and proposed to play an essential role in the formation of PAHs.[29] Note that fulvenallenyl can be generated through the heterolytic C–H dissociation of fulvenallene (C_7H_6) at the terminal methylene group (Scheme 2a)[30–32] by overcoming the thermodynamic barrier of 82.5 kcal mol^{-1} (ref. 32) at a high temperature of ~1000 K in the combustion-like environments of the circumstellar envelopes. It is noteworthy that fulvenallenyl ($C_7H_5^{\bullet}$) can be also produced *via* the photolysis of fulvenallene (C_7H_6) by the internal ultraviolet fields that exist even deep inside molecular clouds such as the Taurus Molecular Cloud-1 (TMC-1),[26] in which abundant fulvenallene ($(2.7 \pm 0.3) \times 10^{-10}$ relative to H_2) has been detected. Theoretical studies indicate that the allenic- and acetylenic-resonant structures (Scheme 2b) are the globally stable ones on the C_7H_5 potential energy surfaces (PESs),[30] with branching ratios of 24% and 76%, respectively.[33] Consequently, fulvenallenyl is believed to be long-lived, which increases the probability of its self-reaction.[28] Although it has already been predicted that PAHs with two or three six-membered rings could be generated through pathways involving fulvenallenyl,[28,34] convincing evidence from experimental or theoretical studies is scarce due to the insurmountable difficulties in preparing sufficiently high concentrations of fulvenallenyl radicals. Notably, the newly reported fulvenallenyl addition cyclization aromatization (FACA) reaction mechanism[35] to form azulene, a PAH that consists of a five- and a seven-membered carbon ring, represents the prologue to rapid prototyping of the formation of planar PAHs and saddle-shaped aromatics through reaction pathways involving fulvenallenyl. It further demonstrates the essential role of fulvenallenyl in barrierless molecular mass growth processes and represents a strategy to prepare sufficient contents of fulvenallenyl to explore its chemical reactions experimentally. In fact, da Silva and Hirsch have proposed that the self-combination of fulvenallenyl radicals could lead to the formation of the $C_{14}H_{10}$ PAH phenanthrene,[28,34] although further experimental and theoretical studies are required to reveal the specific and exhaustive

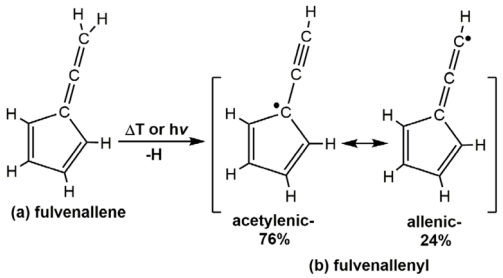

Scheme 2 Fulvenallenyl (a) generated by the pyrolysis of fulvenallene (b).

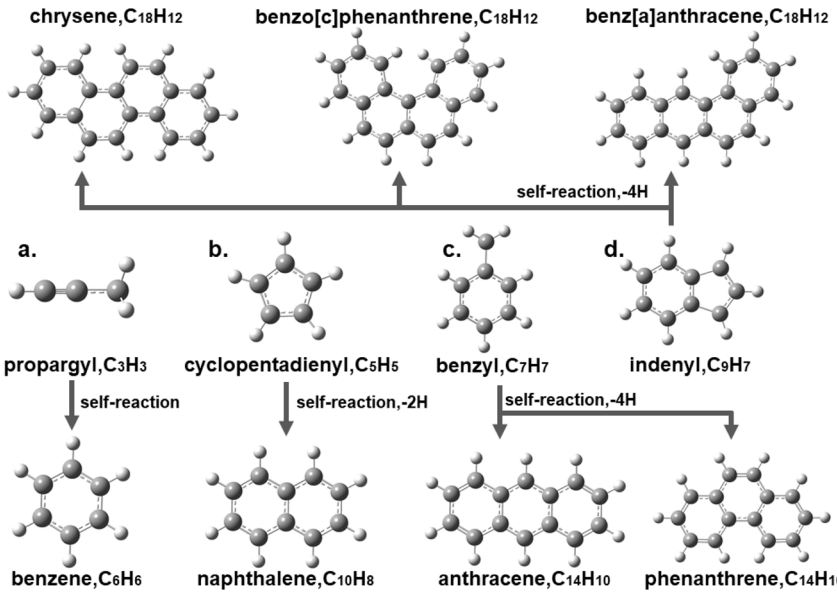

Scheme 1 Representative resonantly stabilized free radicals (RSFRs) and products of the self-reactions of some RSFRs, including (a) propargyl, (b) cyclopentadienyl, (c) benzyl and (d) indenyl. Atoms are color coded in gray (carbon) and white (hydrogen).

recombination mechanisms of fulvenallenyl as a resonance-stabilized radical.

Phenanthrene ($pC_{14}H_{10}$) and anthracene ($aC_{14}H_{10}$), the simplest 14π-representatives of $C_{14}H_{10}$ helicenes and acenes, respectively, have attracted great attention in the areas of interstellar evolution, soot formation and nanoparticle synthesis. Anthracene cations have been observed and identified in the star Cernis 52 ($1.7 \pm 0.4 \times 10^{-9}$ relative to H_2).[36] PAH cations or neutral molecules consisting of three aromatic rings, including anthracene and phenanthrene, are considered likely carriers of UIR emission bands between the wavelengths of 3.3 and 16.4 μm in the interstellar environment,[37] and both of them have been proven to be essential precursors for the growth of PAHs.[38] PAHs containing anthracene and/or phenanthrene configurations are known to have high thermal reactivity[39,40] and a tendency toward nanoparticle formation,[41,42] especially at low temperatures.[38] In addition, both phenanthrene and anthracene are valuable compounds in organic synthesis[43,44] and materials science.[45–47] Their aromaticity[48–50] has made them prevalent as building blocks for the production of more complex organic molecules and the development of various functional materials, such as organic light-emitting diodes (OLEDs) and fluorescent dyes.[51] Phenanthrene and anthracene are also significant environmental pollutants, making them indicator compounds for assessing pollution levels.[52,53] Thus, it is also an urgent task for human beings to reveal their corresponding formation mechanisms to minimize their adverse effects on human health and ecosystems.

This work reports a combined experimental and computational study on the unconventional gas-phase formation mechanisms of fulvenallenyl recombination that eventually lead to phenanthrene ($pC_{14}H_{10}$) and anthracene ($aC_{14}H_{10}$) through the FACA mechanism. A chemical microreactor consisting of a silicon carbide (SiC) tube was adopted in the current work. The reaction products were sampled in a molecular beam and isomer-specifically *via* fragment-free photoionization of the neutral products, exploiting tunable vacuum ultraviolet (VUV) light, followed by detection of the ionized molecules in a reflection time-of-flight mass spectrometer. Using electronic structure calculations, the detailed formation pathways of phenanthrene and anthracene have also been uncovered. The current investigation of fulvenallenyl recombination reveals a novel formation mechanism for the simplest 14π-representatives of helicenes and acenes, which are closely related to carbonaceous nanostructures such as fullerenes, nanocages and nanotubes, and further facilitates an understanding of molecular mass growth processes *via* RSFR recombination.

Results and discussion

Photoionization mass spectra

As the very first step, the mass spectra of a trichloromethylbenzene ($C_7H_5Cl_3$)/helium (He) system were assessed qualitatively. A representative mass spectrum collected at 9.00 eV at a temperature of 1098 ± 10 K (ESI, Section 1†) to explore the self-recombination of fulvenallenyl ($C_7H_5^{\bullet}$) in the $C_7H_5Cl_3$/He system is presented in Fig. 1b. The mass spectrum of the control experiment recorded at 9.00 eV and 373 ± 10 K is also given in Fig. 1a. Only ion peaks corresponding to the precursors at mass-to-charge ratios (m/z) of 194 ($C_7H_5{}^{35}Cl_3^+$), 195 ($^{13}CC_6H_5{}^{35}Cl_3^+$), 196 ($C_7H_5{}^{35}Cl_2{}^{37}Cl^+$), 197 ($^{13}CC_6H_5{}^{35}Cl_2{}^{37}Cl^+$), 198 ($C_7H_5{}^{35}Cl^{37}Cl_2^+$), 199 ($^{13}CC_6H_5{}^{35}Cl^{37}Cl_2^+$) and 200 ($C_7H_5{}^{37}Cl_3^+$) are detected in the $C_7H_5Cl_3$/He system at 373 ± 10 K, whereas all of them disappear at 1098 ± 10 K, indicating the complete decomposition of the precursor $C_7H_5Cl_3$. With the rise

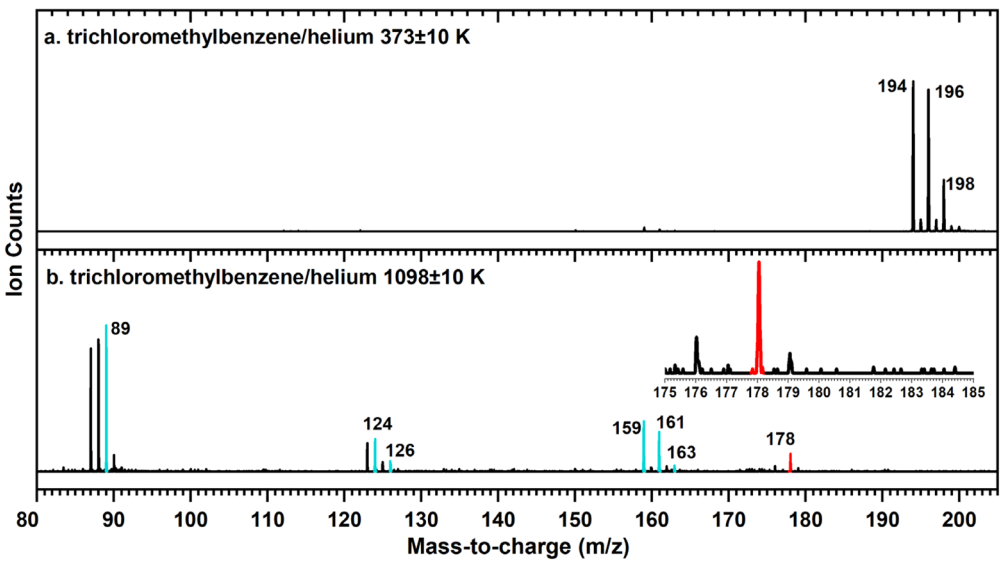

Fig. 1 Photoionization mass spectra to explore fulvenallenyl self-recombination recorded at 9.00 eV for (a) the trichloromethylbenzene ($C_7H_5Cl_3$)/helium (He) system at 373 ± 10 K and (b) the trichloromethylbenzene ($C_7H_5Cl_3$)/helium (He) system at 1098 ± 10 K. The signal of interest in the study (m/z = 178) is highlighted in red. The peaks at m/z = 89, 124, 126, 159, 161 and 163 marked in blue are related to the stepwise loss of Cl from trichloromethylbenzene ($C_7H_5Cl_3$).

of the experimental temperature, the Cl atoms are gradually eliminated from the $C_7H_5Cl_3$ molecule, and the corresponding ion peaks (marked in blue) were observed (Fig. 1b); a detailed description is provided in the ESI (Fig. S1–S3†). Under the experimental conditions, the expected ion peak was observed at $m/z = 178$ ($C_{14}H_{10}^{+}$), which is twice the mass-to-charge ratio of the ionized fulvenallenyl radical ($C_7H_5^{+}$, $m/z = 89$). Thus, it is quite likely that the isomer(s) with the $C_{14}H_{10}$ formula can be attributed to the self-recombination of fulvenallenyl. However, considering the multi-Cl-substituted structure of the precursor, it is also possible that the products at $m/z = 178$ are produced *via* the reaction of C_7H_5Cl ($m/z = 124$, 126) or $C_7H_5Cl_2^{\bullet}$ ($m/z = 159$, 161, 163) radicals with fulvenallenyl. However, ion peaks at $m/z =$ 213, 215, 248, 250 and 252, which would correspond to the direct addition products of C_7H_5Cl ($m/z = 124$, 126) or $C_7H_5Cl_2^{\bullet}$ ($m/z =$ 159, 161, 163) radicals with fulvenallenyl, were not detected (ESI Fig. S4†), thus excluding these potential reaction channels. Additionally, the possible pathways for the generation of the products at $m/z = 178$ *via* self-recombination of C_7H_5Cl ($m/z =$ 124, 126) or $C_7H_5Cl_2^{\bullet}$ ($m/z = 159$, 161, 163) intermediates followed by stepwise Cl-elimination were also ruled out based on the absence of signals at $m/z = 248$, 252, 318, 322 and 326 (ESI Fig. S4†). It also should be noted that the intensity of collected ions at $m/z = 90$ is about 9.15% that at $m/z = 89$ (Fig. 1b), suggesting the ion peak at $m/z = 89$ primarily originates from ^{13}C isotopes (7 × 1.109% natural abundance) of C_7H_5 isomers, which can be further verified from ESI Fig. S1c.† Hence, the molecule–radical reaction of C_7H_6 (90 amu) and C_7H_5 (89 amu) is assumed to have a negligible contribution to the $C_{14}H_{10}$ (178 amu) signal. As a result, it was concluded that the isomer(s) with the formula $C_{14}H_{10}$ are predominantly generated from the self-recombination reaction of fulvenallenyl.

Photoionization efficiency (PIE) curves

This work focuses on the signal at $m/z = 178$ ($C_{14}H_{10}$), which is related to the tricyclic products of the fulvenallenyl recombination. To further identify the chemical structures of the $C_{14}H_{10}$ isomer(s) formed in the experimental system, an in-depth analysis of the corresponding photoionization efficiency (PIE) curves (Fig. 2) plotting the ion count at $m/z = 178$ as a function of photon energy from 7.00 to 9.00 eV is required. The photoionization efficiency (PIE) curves were measured at intervals of 0.05 eV from 7.00 to 9.00 eV at 1098 ± 10 K. The onset value of the experimental PIE curve at $m/z = 89$ (Fig. 2a) is 8.20 ± 0.03 eV, which agrees exceptionally well with the ionization energy (IE = 8.19 eV)[31] of fulvenallenyl ($C_7H_5^{\bullet}$), and the trend in the experimental PIE data agrees well with that of fulvenallenyl generated from the pyrolysis of the 'traditional' phthalide precursor[31,34] (ESI Fig. S5–S8†), which provides convincing evidence for the generation of fulvenallenyl from the decomposition of trichloromethylbenzene ($C_7H_5Cl_3$) at 1098 ± 10 K. As shown in Fig. 2b, the experimental PIE data at $m/z = 178$ can be nicely replicated using a linear combination of the reference/calculated curves of anthracene, phenanthrene and two other $C_{14}H_{10}$ isomers, 3,4-di(cyclopenta-2,4-dien-1-ylidene)cyclobut-1-ene and 1-(cyclopenta-2,4-dien-1-ylidene)indene. The first onset value of the experimental PIE curve at $m/z = 178$ is 7.45 ± 0.03 eV, which agrees exactly with the IE (7.44 eV)[54] of

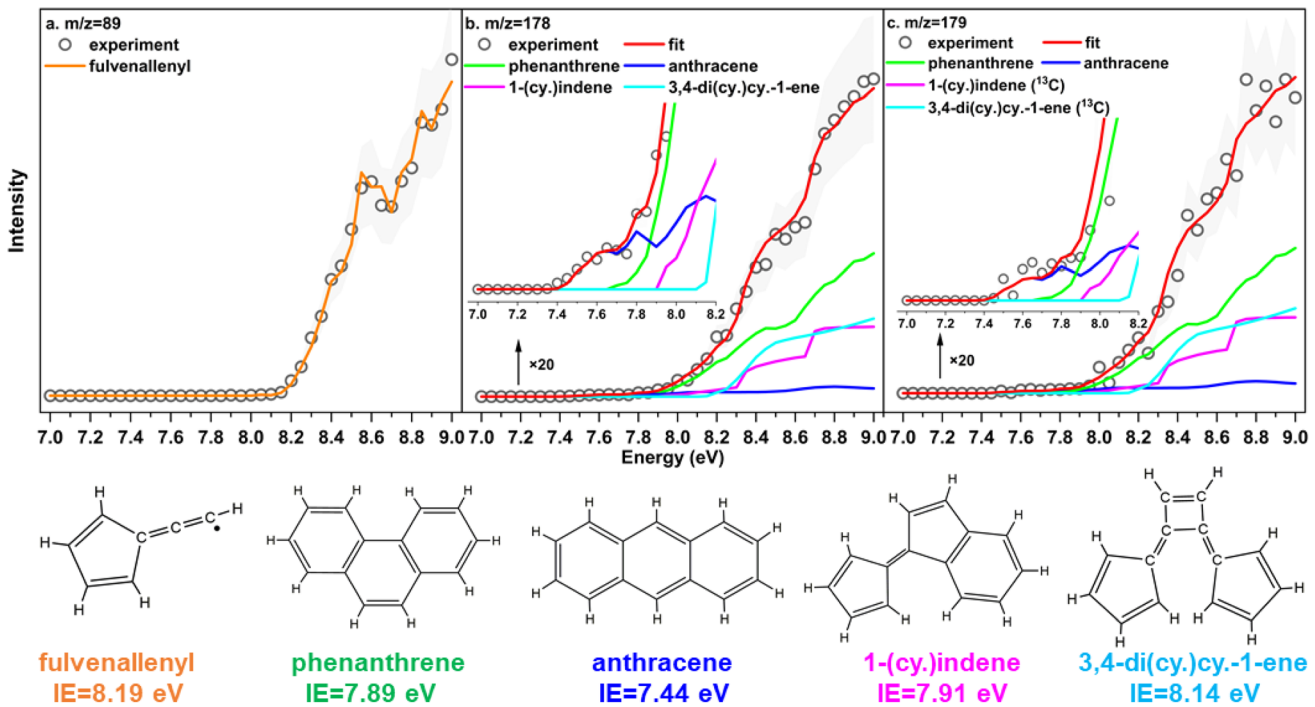

Fig. 2 Experimental and reference PIE curves for species at m/z = (a) 89, (b) 178 and (c) 179 in a trichloromethyl–benzene ($C_7H_5Cl_3$)/helium (He) system at 1098 ± 10 K. The black circles represent the experimental data, with 1σ error limits defined by the shaded area. The colored lines represent the reference PIE curves of the isomers. The red line shows the overall fit *via* the linear combination of the reference curves.

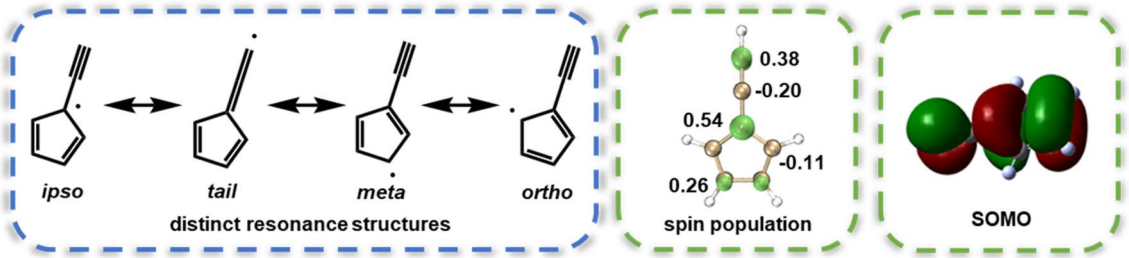

Fig. 3 Distinct resonance structures, spin density (isosurface = 0.02), and singly occupied molecular orbital (SOMO) of the fulvenallenyl radical calculated at the B3LYP-D3(BJ)/6-311+G(d,p) level.

anthracene. Additionally, a contribution from phenanthrene (IE = 7.89 eV)[54] is required at 7.90 ± 0.03 eV to match the total fitting of the experimental PIE curve. However, the experimental PIE curve of $m/z = 178$ is not well fitted over the whole energy range of 7.00–9.00 eV using only the standard photoionization cross sections (PICSs) of anthracene and phenanthrene (ESI Fig. S9a†), which indicates the existence of other $C_{14}H_{10}$ isomers. Thus, two $C_{14}H_{10}$ isomers whose PICS were calculated in this work (ESI, Section 1†), 3,4-di(cyclopenta-2,4-dien-1-ylidene)cyclobut-1-ene (IE = 8.14 eV, ESI Table S1†) and 1-(cyclopenta-2,4-dien-1-ylidene)indene (IE = 7.91 eV, ESI Table S1†), were added to the fitting, and comparisons among the results of fittings using distinct $C_{14}H_{10}$ PICSs (Fig. 3 and ESI Fig. S9†) confirm the coexistence of 3,4-di(cyclopenta-2,4-dien-1-ylidene)cyclobut-1-ene and 1-(cyclopenta-2,4-dien-1-ylidene) indene. The rationale for selecting these two specific isomers from among the various possible $C_{14}H_{10}$ molecules for the PIE fitting will be discussed later. The fitting results for the experimental PIE in the energy range of 7.00 to 9.00 eV clearly indicate the formation of four $C_{14}H_{10}$ isomers, namely, anthracene, phenanthrene, 3,4-di(cyclopenta-2,4-dien-1-ylidene)cyclobut-1-ene and 1-(cyclopenta-2,4-dien-1-ylidene)indene, with branching ratios of 0.31 : 90.83 : 3.13 : 5.73% accounting for corresponding photoionization cross sections of 15.1, 5.8, 34.1 and 22.3 Mb at 8.50 eV,[54] in the fulvenallenyl self-recombination reaction system under the current experimental conditions (1098 ± 10 K, ~100 Torr). The outcome of the fitting of the experimental PIE curve for the peak at $m/z = 179$ resulting from the ^{13}C isotopes (14 × 1.109% natural abundance) of the $C_{14}H_{10}$ isomers (Fig. 3c) further confirms the syntheses of anthracene, phenanthrene, 3,4-di(cyclopenta-2,4-dien-1-ylidene)cyclobut-1-ene and 1-(cyclopenta-2,4-dien-1-ylidene)indene in the fulvenallenyl self-reaction system. A previous investigation of fulvenallenyl self-recombination using infrared (IR)/ultraviolet (UV) ion dip spectroscopy merely identified phenanthrene, but did not give precise evidence of the existence of anthracene or other potential isomers,[34] possibly due to the sensitivity limit of the IR/UV detection method for low-yield products (less than 10%). The detailed formation mechanism of these detected $C_{14}H_{10}$ species was further studied theoretically.

Recombination of fulvenallenyl radicals

The spin density and singly occupied molecular orbital (SOMO) of the fulvenallenyl radical calculated using Multiwfn[55] (Fig. 3) reveal that the unpaired electron is mainly localized around the *ipso* site of the carbon ring, followed by the *tail* site and the *meta* site, suggesting that the radical–radical recombination tends to

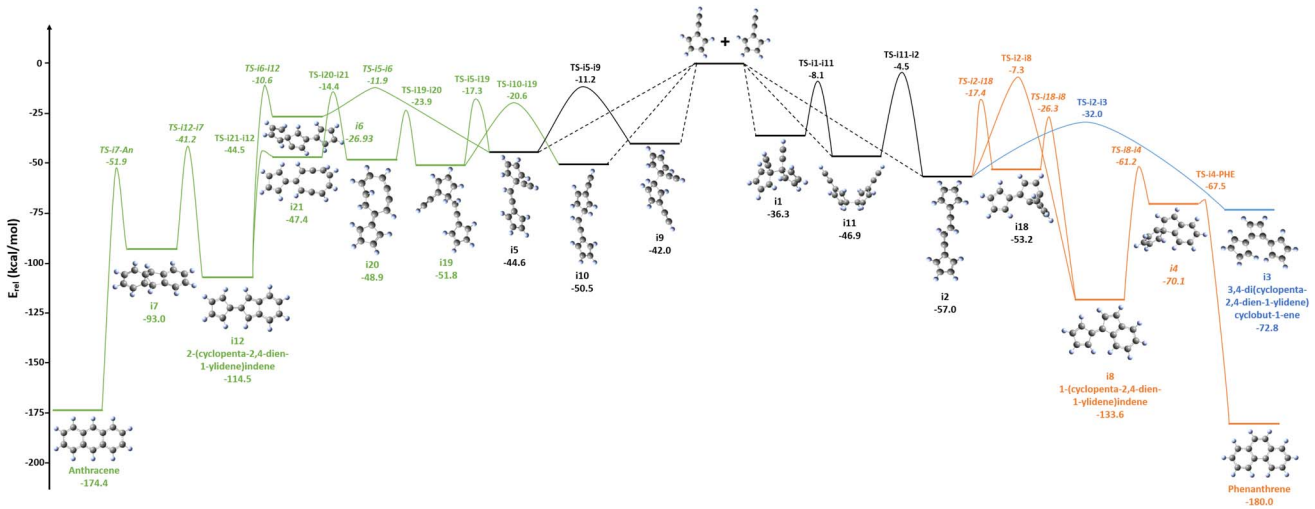

Fig. 4 PESs (in kcal mol^{-1}) of fulvenallenyl radical self-recombination reaction leading to various isomers of $C_{14}H_{10}$. The initial addition pathways and isomerization pathways to phenanthrene, anthracene, and i3 are shown in black, orange, green, and blue, respectively.

be initiated through the rapid additions of these carbon sites. Conversely, the unpaired electron is rarely distributed around the *ortho* site, indicating its lower reactivity for the radical–radical addition process. Fig. 4 illustrates the relative energies of the key isomers on the fulvenallenyl self-reaction potential energy surface, including various direct adducts (*ipso–ipso* adduct i1, *tail–tail* adduct i2, *ipso–tail* adduct i5, *ipso–meta* adduct i9, *tail–meta* adduct i10, and *meta–meta* adduct i11), the vital intermediates [1-(cyclopenta-2,4-dien-1-ylidene)indene (i8) and i12, *etc.*] and the products [phenanthrene, 3,4-di(cyclopenta-2,4-dien-1-ylidene)cyclobut-1-ene (i3), and anthracene]. The calculation details can be found in the ESI (Section 1†). Although direct additions involving the *ortho* site carbon are seemingly unable to compete with the above adducts, the *tail–ortho* adduct i19 (-51.8 kcal mol^{-1}) can be formed by the migrations of the C_2H moiety of i5 (-44.6 kcal mol^{-1}) and i10 (-50.5 kcal mol^{-1}), with submerged barriers of 27.4 kcal mol^{-1} and 29.9 kcal mol^{-1}, respectively. Among these initial adducts, i2 (-57.0 kcal mol^{-1}) is the most stable one, with an energy 20.7 kcal mol^{-1} lower than that of the most unstable adduct i1 (-36.3 kcal mol^{-1}). Overall, the initial adducts can be roughly divided into two addition groups (i5 + i9 + i10/i1 + i2 + i11), where the adducts cannot be directly converted to wells in the other group. Other conformers of these adducts that can be easily obtained from the most stable conformers *via* low-barrier (<10 kcal mol^{-1}) rotation around a single bond are listed in ESI Fig. S10.†

As shown in Fig. 4, the adducts i2, i5, and i10 will undergo different two-stage ring-enlargement processes, which eventually lead to thermally stable phenanthrene (-180.0 kcal mol^{-1}) and anthracene (-174.4 kcal mol^{-1}), respectively. In the first stage, the highly stable intermediates i8 [1-(cyclopenta-2,4-dien-1-ylidene)indene, -133.6 kcal mol^{-1}] and i12 [2-(cyclopenta-2,4-dien-1-ylidene)indene, -114.5 kcal mol^{-1}] are formed through multi-step cyclization (i2 → i18 → i8, i5 → i6 → i12, i10/i5 → i19 → i20 → i21 → i12) and one-step (i2 → i8) cyclization of the non-cyclic chain parts of i2 or i5/i10, respectively. Compared with the isomerization processes to form i12, the formation of i8 is more energetically favorable, which is consistent with the identification of i8 in the present experiment. The second stage of the ring-enlargement process from i8 to phenanthrene and from i12 to anthracene predominantly involves a spiran-like mechanism, which is similar to the spiran mechanism proposed in previous theoretical investigations into C_5H_5–C_5H_6, C_5H_5–C_5H_5, and C_9H_7–C_5H_5 reactions.[56–58] It must be noted that the H-assisted isomerization from i12 or i8 is a competitive channel for phenanthrene and anthracene formation; detailed information can be found in the study of the reaction of indenyl ($C_9H_7^{\bullet}$) with cyclopentadienyl ($C_5H_5^{\bullet}$) by He *et al.*[57] Their theoretical calculations revealed that the reaction between i8 and a hydrogen atom is an accessible and prevalent route to produce phenanthrene and anthracene as the major and minor products in a hydrogen-rich environment.[57]

In addition to the above isomerization routes leading to phenanthrene and anthracene, a $C_{14}H_{10}$ product with two five-membered rings and one four-membered ring, i3 [3,4-di(cyclopenta-2,4-dien-1-ylidene)cyclobut-1-ene, -72.8 kcal mol^{-1}], can be also formed *via* the isomerization of i2. The calculations of the $C_{14}H_{10}$ PES show that i3, with a much lower barrier (25.0 kcal mol^{-1}), is a more energetically favorable product compared with i8, phenanthrene and anthracene. However, the much higher relative energy (-72.8 kcal mol^{-1}) of i3 hinders its competitiveness with phenanthrene under the thermally preferred conditions, which may be the main cause for i3 not being detected under the previous experimental conditions with a much longer residence time.[34] Several other isomerization pathways from i2 were also observed (ESI Fig. S11†), which would produce i14 and i17, respectively. The two isomers (i14 and i17) cannot compete with phenanthrene under dynamically or thermally preferred conditions due to their higher barriers and enthalpies. Overall, under the experimental conditions (1098 ± 10 K, ∼100 Torr), i3 is deemed to be the dominant product of the recombination reaction of fulvenallenyl radicals ($C_7H_5^{\bullet}$ + $C_7H_5^{\bullet}$ → i3) in the theoretical calculation. However, the deviation between the theoretical calculation and the experimental results (only 3.13% of the products at $m/z = 178$) indicates the existence of an efficient secondary reaction from i3 leading to anthracene or phenanthrene. Based on the PES of $C_7H_5^{\bullet}$ recombination (Fig. 4) and the ionization energies of $C_{14}H_{10}$ species (ESI Table S1†), it is thought that the i3 and i8 structures might contribute to the $C_{14}H_{10}$ product pool. Thus, the standard PICSs of these two isomers were newly calculated and used to fit the experimental data, and a satisfactory overall fitting was obtained, as mentioned above.

H-assisted isomerization of i3 to phenanthrene and anthracene

Both C_7H_5Cl (124 and 126 amu) and C_7H_5 (89 amu) can undergo further H-elimination at high experimental temperature,[59] which led to the detection of ion peaks at 123, 125 and 88 amu (Fig. 1) and consequently results in a hydrogen-enriched atmosphere in the studied reaction system. The H-assisted isomerization from a five-membered ring to a six-membered ring (A5 to A6 H-assisted mechanism) has been proven to be efficient,[60] and it has also been proven that H atoms are efficiently generated in the trichloromethylbenzene thermal decomposition system;[35] thus, H-assisted isomerization might play a significant role in this system. Therefore, the feasibility of an H-assisted ring-enlargement mechanism from i3 to phenanthrene and anthracene was further studied using theoretical calculations. Fig. 5 shows the PESs of the H-assisted mechanisms of i3 calculated in this work, which lead to different $C_{14}H_{11}$ wells and $C_{14}H_{10}$ + H bimolecular products. Firstly, by overcoming barriers ranging from 6.9 to 8.5 kcal mol^{-1}, a hydrogen atom could potentially add to each unsaturated carbon site of i3, resulting in the diverse addition routes (add1–add7) shown in ESI Fig. S12.† After the initial addition, two different spiran structures (P5 and P6) would be formed from add1 and add2 through three-membered ring structures P2 and P3, respectively, which would further cyclize to the wells partly with indene-like structures and eliminate H atoms to form i8, B2, B1, phenanthrene, and anthracene. Notably, the PES for i3 + H to i8 + H (i3 + H → i8 + H) shown in Fig. 5a and b is connected to the PES from i8 + H to

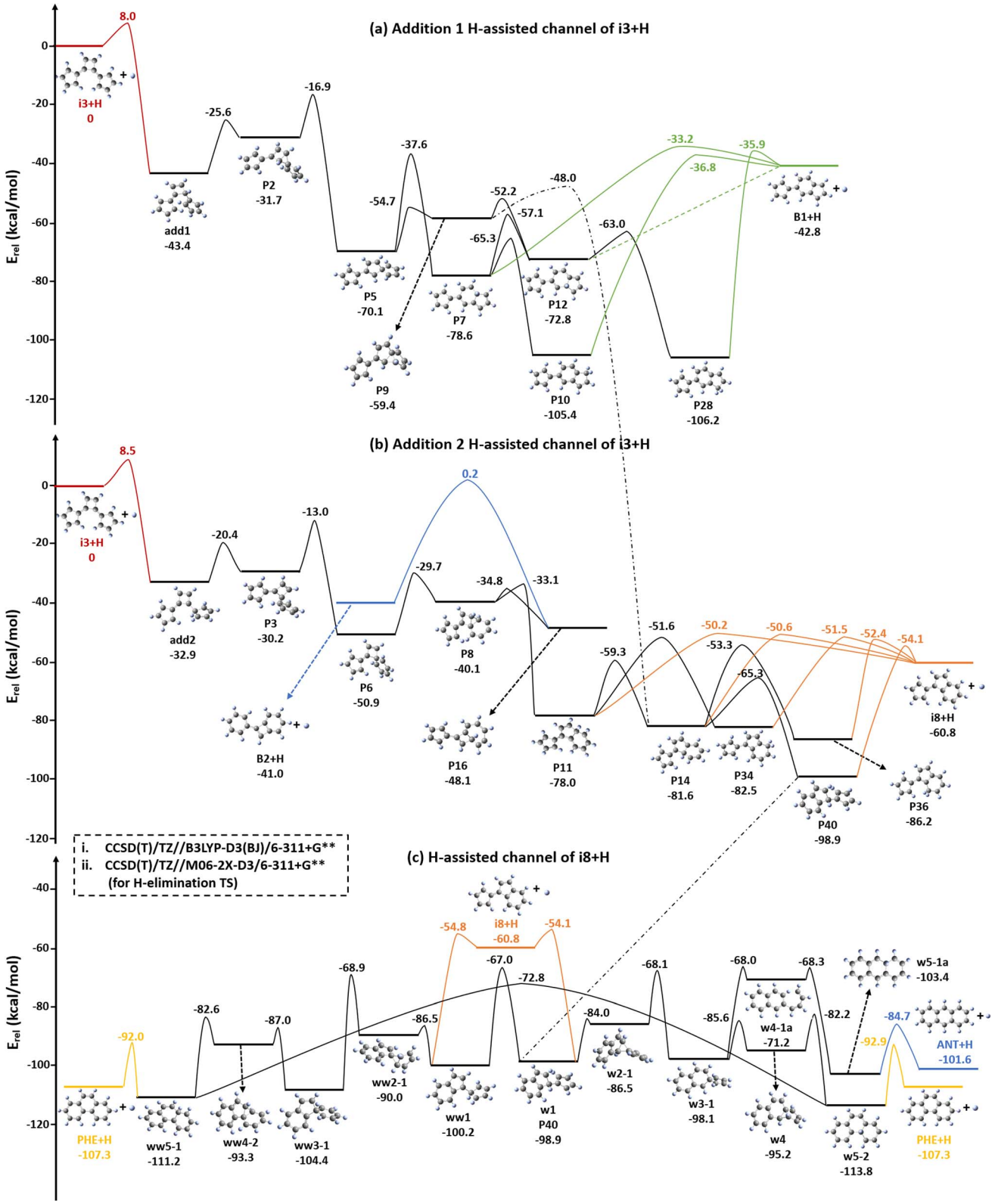

Fig. 5 PESs (in kcal mol^{-1}) of isomerization channels of (a) add1, (b) add2, and (c) i8 + H for the H-assisted reactions between i3 and hydrogen atoms leading to various $C_{14}H_{11}$ isomer wells and $C_{14}H_{10}$ + H bimolecular products. The initial addition pathways, isomerization pathways, and H-elimination channels are shown in red, black, and other colors, respectively.

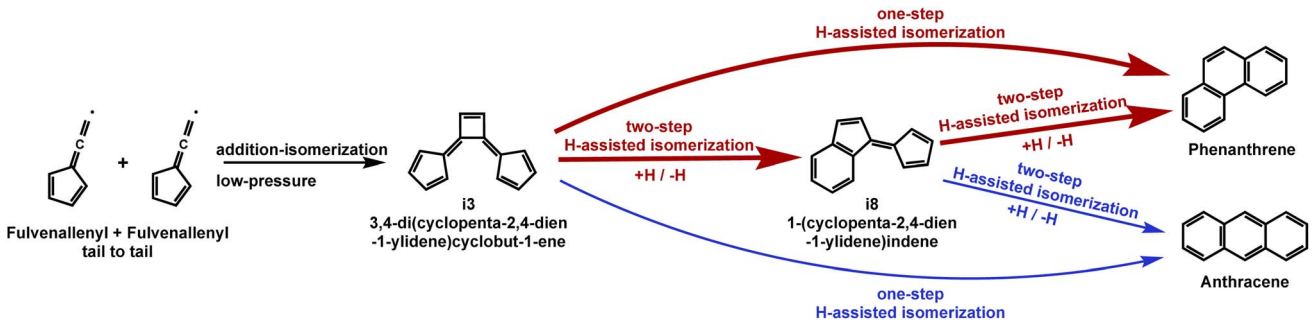

Fig. 6 Schematic representation of formation mechanisms to give phenanthrene and anthracene under the studied conditions.

phenanthrene + H or anthracene + H (i8 + H → phenanthrene + H/anthracene + H) through the "bridge" intermediate P40 (Fig. 5b and c), suggesting the potential feasibility of converting the high-energy i3 + H complex directly to phenanthrene + H or anthracene + H (i3 + H → phenanthrene + H/anthracene + H) *via* the one-step well-skipping pathway[61] without going through the isomerization of i3 + H to i8 + H. The general procedure for the H-assisted isomerization from the four-membered ring (i3) to the five-membered ring (i8) is similar to that from a five-membered ring to a six-membered ring.[62] The geometries from i8 to phenanthrene and anthracene with hydrogen assistance (Fig. 5c) mainly refer to the previous calculations of Krasnoukhov *et al.*,[63] while the energies were refined using the more precise CCSD(T)/cc-pVTZ method (ESI Fig. S13†). This work has theoretically proven that the H-assisted isomerization of i8 results in considerable conversion of i8 to phenanthrene (~99%) (i8 + H → phenanthrene + H) with a high rate coefficient of $\sim 10^{-11}$ cm^3 per molecule per s, accompanied by minor generation of anthracene (~1%) (i8 + H → anthracene + H). The H-elimination barriers to phenanthrene are ~8.0 kcal mol^{-1} lower than that to anthracene, so it is predicted here that the formation of phenanthrene will be overwhelmingly preferred over the formation of anthracene, which is validated by the relative abundance of these two species in the present experiments. At high pressures, the collisional stabilization of $C_{14}H_{11}$ adducts may become more important for the H-assisted reaction of i3, whereas at the experimental low pressures (~100 Torr), the biomolecular products (i8 + H, phenanthrene + H, or anthracene + H) will exhibit higher branching ratios, as discussed in the study of an analogous reaction between hydrogen and fulvene.[60] Overall, our results generally show the feasibility of the H-assisted ring-enlargement mechanisms from i3 to phenanthrene and anthracene, and the two candidate mechanisms presented in Fig. 6 are summarized here:

i3 + H → phenanthrene/anthracene + H (R1, one-step H-assisted ring-enlargement)

i3 + H → i8 + H → phenanthrene/anthracene + H (R2, two-step H-assisted ring-enlargement)

Considering the relatively high efficiency of producing i3 from the fulvenallenyl recombination reaction at low pressures, these mechanisms should be efficient and play an integral role in the formation of tricyclic aromatics from the fulvenallenyl radicals. Additionally, this work calls attention to the lack of understanding of the H-assisted mechanism from four-membered rings to five-/six-membered rings in the model for PAH weight growth.

Additionally, abundant chlorine atoms are also generated in the trichloromethylbenzene-based experiment at elevated temperature, and it is emphasized that the majority of the chlorine (Cl) atoms are stabilized as diatomic molecules (Cl_2) prior to reaching the aromatic growth reaction stage.[64,65] Chlorine-assistance was also considered; however, no significant signal for $C_{14}H_9Cl$, one of the potential Cl-assisted products (Fig. S14†), was detected at $m/z = 212$ or 214 in the current experiments (Fig. S4†), suggesting that the Cl-assisted mechanism is highly inefficient under the experimental conditions and can thus be disregarded. Additionally, a similar $C_{14}H_{10}$ signal was also observed (Fig. S6†) in phthalide-based experiments conducted in the absence of chlorine atoms, which further indicates that chlorine assistance exerts a negligible influence on the isomerization of the primary $C_{14}H_{10}$ products to phenanthrene and anthracene.

Conclusions and outlook

Experiments with a short residence time to investigate of self-recombination reaction of the typical resonantly stabilized free radical, fulvenallenyl ($C_7H_5^{\bullet}$), provided convincing evidence of the syntheses of phenanthrene ($pC_{14}H_{10}$) as the major product and anthracene ($aC_{14}H_{10}$) as a minor product, along with the intermediates i3 [3,4-di(cyclopenta-2,4-dien-1-ylidene) cyclobut-1-ene] and i8 [1-(cyclopenta-2,4-dien-1-ylidene) indene]. Based on theoretical calculations, phenanthrene and anthracene are thought to form *via* a multi-step mechanism rather than the direct well-skipping addition–isomerization reaction of fulvenallenyl ($C_7H_5^{\bullet}$). On the PES of the fulvenallenyl + fulvenallenyl reaction, the reactant, fulvenallenyl, first undergoes a rapid and barrierless radical–radical recombination process, leading to the formation of various adducts. Six diverse entrance channels were considered based on the evaluation of the spin density of fulvenallenyl molecule, including terminal CH addition to the terminal CH or the C atoms at the ring, and additions among the C atoms at the ring. The addition between two terminal CH groups forms the vital immediate, i2,

in the self-reaction system of fulvenallenyl, eventually leading to the formation of abundant i3 under the experimental conditions ($C_7H_5^{\bullet}$ + $C_7H_5^{\bullet}$ → i3). Subsequently, i3 reacts with a hydrogen atom to produce mainly phenanthrene and with a minor amount of anthracene *via* a one-step H-assisted isomerization (i3 + H → $aC_{14}H_{10}$ + H/$pC_{14}H_{10}$ + H) or a two-step H-assisted isomerization (i3 + H → i8 + H; i8 + H → $aC_{14}H_{10}$ + H/$pC_{14}H_{10}$ + H), as shown in Fig. 6. Calculation of the reaction of i3 and a hydrogen atom also indicated the omission of H-assisted ring-enlargement from four-membered rings to five-/six-membered rings in the widely-used mechanism for PAH growth. The addition barriers for the four-membered H-assisted isomerization are several kcal mol^{-1} higher than those for the five-membered H-assisted one in this work. In conclusion, the current work has explored the chemical self-reactions of typical RSFRs and confirmed the close relevance between RSFRs and PAHs, further revealing a novel molecular-weight growth pathway for two common PAHs, phenanthrene and anthracene, in combustion flame, interstellar and industrial synthesis environments.

Two PAH products of great interest, phenanthrene and anthracene, along with other $C_{14}H_{10}$ isomers, were proven to be generated through the recombination processes of the fulvenallenyl radical *via* an unexpected submerged barrierless multi-step mechanism. In circumstellar environments, barrierless molecular-weight growth channels of PAHs are highly effective,[54,57] and hydrogen-rich environments also allow for rapid isomerization towards the two stable products phenanthrene and anthracene. This efficient mechanism is feasible not only in flame conditions including combustion processes and the circumstellar envelopes[26] but also potentially in low-temperature environments. The formation mechanisms of the PAH sinks detected in low-temperature atmospheres like that of Titan (3.28 μm by Cassini's VIMS)[66] have long been a critical puzzle. It was previously reported that phenanthrene and anthracene can be also generated through other RSFR–RSFR pathways, including indenyl ($C_9H_7^{\bullet}$)–cyclopentadienyl ($C_5H_5^{\bullet}$) reaction,[57] the reaction of naphthyl ($C_{10}H_7^{\bullet}$) with vinylacetylene (C_4H_4) *via* the hydrogen-abstraction–vinylacetylene-addition (HAVA) mechanism,[67] and benzyl ($C_7H_7^{\bullet}$)–benzyl ($C_7H_7^{\bullet}$) reaction,[54] with barrierless entrance channels. However, the high reaction barriers in the global PESs rule out the possibility of the formation of $C_{14}H_{10}$ aromatics from benzyl ($C_7H_7^{\bullet}$) recombination[54] or the reaction of indenyl ($C_9H_7^{\bullet}$) with cyclopentadienyl ($C_5H_5^{\bullet}$)[57] under low-temperature conditions. Toluene (C_7H_8), which has been detected in Titan's atmosphere,[68] could generate fulvenallenyl radicals *via* successive H-elimination processes (toluene → benzyl ($C_7H_7^{\bullet}$) → fulvenallene → fulvenallenyl) *via* solar ultraviolet photolysis,[69,70] further contributing to the formation of $C_{14}H_{10}$ aromatic products. In addition, barrierless molecular mass growth routes, including the reaction of benzene (C_6H_6) with methylidyne (CH)[71] and the reaction of *ortho*-benzyne (C_6H_4) with methyl (CH_3),[72] are believed to be the essential channels of fulvenallenyl generation in planetary and interstellar environments. Thus, these crucial data represent a possible explanation of how they can be linked to the haze layers, ultimately providing an alternative potential low-temperature PAH formation route, *i.e.*, the FACA mechanism, in addition to the previous hydrogen-abstraction–vinylacetylene-addition (HAVA) pathways.[67] In conclusion, our comprehensive experimental and computational study provides a template for the needed investigation of the PAH chemistry in cold conditions TMC-1 and planetary and satellite atmospheres such as that of Titan.

Data availability

Essential data are provided in the main text and the ESI.† Additional data are available from the corresponding author upon reasonable request.

Author contributions

L. Z. designed the experiments; W. L. and C. W. carried out the experimental measurements in NSRL and performed the data analysis; L. Z. and T. Y. supervised the experiments; M. W. and J. H. carried out the theoretical analysis; F. Z. supervised the theoretical analysis; all authors discussed the data; W. L. and M. W. wrote the manuscript draft. All authors reviewed and edited the manuscript.

Conflicts of interest

The authors declare no competing interest.

Acknowledgements

The authors are grateful for the funding supports from National Natural Science Foundation of China (22173091) and the Innovation Program for Quantum Science and Technology (2021ZD0303303). T. Y. thanks the support from the Xinjiang Tianchi Talent Program (2023).

References

1 H. Jin, W. Yuan, W. Li, J. Yang, Z. Zhou, L. Zhao, Y. Li and F. Qi, Combustion chemistry of aromatic hydrocarbons, *Prog. Energy Combust. Sci.*, 2023, **96**, 101076.
2 Q. Wang, X. Shi, X. Zhang, C. Shao and S. M. Sarathy, Chemistry of nitrogen-containing polycyclic aromatic formation under combustion conditions, *Combust. Flame*, 2023, **249**, 112629.
3 M. López-Puertas, B. M. Dinelli, A. Adriani, B. Funke, M. García-Comas, M. L. Moriconi, E. D'Aversa, C. Boersma and L. J. Allamandola, Large abundances of polycyclic aromatic hydrocarbons in Titan's upper atmosphere, *Astrophys. J.*, 2013, **770**, 132–140.
4 R. I. Kaiser and N. Hansen, An aromatic universe-a physical chemistry perspective, *J. Phys. Chem. A*, 2021, **125**, 3826–3840.
5 S. Doddipatla1, G. R. Galimova, H. Wei, A. M. Thomas, C. He, Z. Yang, A. N. Morozov, C. N. Shingledecker, A. M. Mebel and R. I. Kaiser, Low-temperature gas-phase formation of indene in the interstellar medium, *Sci. Adv.*, 2021, **7**, eabd4044.

6 D. S. Parker, F. Zhang, Y. S. Kim, R. I. Kaiser, A. Landera, V. V. Kislov, A. M. Mebel and A. G. Tielens, Low temperature formation of naphthalene and its role in the synthesis of PAHs (polycyclic aromatic hydrocarbons) in the interstellar medium, *Proc. Natl. Acad. Sci. U.S.A.*, 2012, **109**, 53–58.

7 G. Wenzel1, I. R. Cooke, P. B. Changala, E. A. Bergin, S. Zhang, A. M. Burkhardt, A. N. Byrne, S. B. Charnley, M. A. Cordiner, M. Duffy, Z. T. P. Fried, H. Gupta, M. S. Holdren, A. Lipnicky, R. A. Loomis, H. T. Shay, C. N. Shingledecker, M. A. Siebert, D. A. Stewart, R. H. J. Willis, C. Xue1, A. J. Remijan, A. E. Wendlandt, M. C. McCarthy and B. A. McGuire, Detection of interstellar 1-cyanopyrene: a four-ring polycyclic aromatic hydrocarbon, *Science*, 2024, **386**, 810–813.

8 P. Ferrari, A. K. Lemmens and B. Redlich, Infrared bands of neutral gas-phase carbon clusters in a broad spectral range, *Phys. Chem. Chem. Phys.*, 2024, **26**, 12324–12330.

9 K. Taniguchi, P. Gorai and J. C. Tan, Carbon-chain chemistry in the interstellar medium, *Astrophys. Space Sci.*, 2024, **369**, 2–41.

10 M. Frenklach and E. D. Feigelson, Formation of polycyclic aromatic hydrocarbons in circumstellar envelopes, *Astrophys. J.*, 1989, **341**, 372–384.

11 I. Cherchneff, The formation of polycyclic aromatic hydrocarbons in evolved circumstellar environments, *EAS Publ. Ser.*, 2011, **46**, 177–189.

12 R. K. Anand, S. Rastogi and B. Kumar, PAH emission features in star-forming regions and late type stars, *J. Astrophys. Astron.*, 2023, **47**, 44–47.

13 A. G. G. M. Tielens, C. Kerckhoven and E. Peeters, Astrochemistry: from molecular clouds to planetary systems, *Proc. IAU Symp.*, 2000, **197**, 349–362.

14 S. Kwok, The mystery of unidentified infrared emission bands, *Astrophys. Space Sci.*, 2022, **367**, 2–12.

15 N. L. J. Cox, The PAH-DIB Hypothesis, *EAS Publ. Ser.*, 2011, **46**, 349–354.

16 F. Salama, G. A. Galazutdinov, J. Krełowski, L. Biennier, Y. Beletsky and I. Song, Polycyclic aromatic hydrocarbons and the diffuse interstellar bands: a survey, *Astrophys. J.*, 2011, **728**, 154–162.

17 K. Fujishima, S. Dziomba, H. Yano, S. I. Kebe, M. Guerrouache, B. Carbonnier and L. J. Rothschild, The non-destructive separation of diverse astrobiologically relevant organic molecules by customizable capillary zone electrophoresis and monolithic capillary electrochromatography, *Int. J. Astrobiol.*, 2019, **18**, 562–574.

18 S. S. Zeichner, J. C. Aponte, S. Bhattacharjee, G. Dong, A. E. Hofmann and J. P. Dworkin, Polycyclic aromatic hydrocarbons in samples of Ryugu formed in the interstellar medium, *Science*, 2023, **382**, 1411–1416.

19 H. Wang, J. Guan, J. Gao, J. Zhang, Q. Xu, G. Xu, L. Jiang, L. Xing, D. G. Truhlar and Z. Wang, Direct observation of covalently bound clusters in resonantly stabilized radical reactions and implications for carbonaceous particle growth, *J. Am. Chem. Soc.*, 2024, **146**, 13571–13579.

20 D. E. Couch, A. J. Zhang, C. A. Taatjes and N. Hansen, Experimental observation of hydrocarbon growth by resonance-stabilized radical-radical chain reaction, *Angew. Chem., Int. Ed.*, 2021, **60**, 27230–27235.

21 K. O. Johansson1, M. P. Head-Gordon, P. E. Schrader, K. R. Wilson and H. A. Michelsen, Resonance-stabilized hydrocarbonradical chain reactions may explain soot inception and growth, *Science*, 2018, **361**, 997–1000.

22 L. Zhao, W. Lu, M. Ahmed, M. V. Zagidullin, V. N. Azyazov, A. N. Morozov, A. M. Mebel and R. I. Kaiser, Gas-phase synthesis of benzene via the propargyl radical self-reaction, *Sci. Adv.*, 2021, **7**, eabf0360.

23 R. I. Kaiser, L. Zhao, W. Lu, M. Ahmed, M. V. Zagidullin, V. N. Azyazov and A. M. Mebel, Formation of benzene and naphthalene through cyclopentadienyl-mediated radical-radical reactions, *J. Phys. Chem. Lett.*, 2022, **13**, 208–213.

24 H. Jin, L. Xing, J. Hao, J. Yang, Y. Zhang, C. Cao, Y. Pan and A. Farooq, A chemical kinetic modeling study of indene pyrolysis, *Combust. Flame*, 2019, **206**, 1–20.

25 M. C. McCarthy, K. L. K. Lee, R. A. Loomis, A. M. Burkhardt, C. N. Shingledecker, S. B. Charnley, M. A. Cordiner, E. Herbst, S. Kalenskii, E. R. Willis, C. Xue, A. J. Remijan and B. A. McGuire, Interstellar detection of the highly polar five-membered ring cyanocyclopentadiene, *Nature Astronomy*, 2020, **5**, 176–180.

26 J. Cernicharo, R. Fuentetaja, M. Agúndez, R. I. Kaiser, C. Cabezas, N. Marcelino, B. Tercero, J. R. Pardo and P. d. Vicente, Discovery of fulvenallene in TMC-1 with the QUIJOTE line survey, *Astron. Astrophys.*, 2022, **663**, L9.

27 L. Zhao, R. I. Kaiser, W. Lu, B. Xu, M. Ahmed, A. N. Morozov, A. M. Mebel, A. H. Howlader and S. F. Wnuk, Molecular mass growth through ring expansion in polycyclic aromatic hydrocarbons via radical-radical reactions, *Nat. Commun.*, 2019, **10**, 3689.

28 G. da Silva and J. W. Bozzelli, The C_7H_5 fulvenallenyl radical as a combustion intermediate: potential new pathways to two- and three-ring PAHs, *J. Phys. Chem. A*, 2009, **113**, 12045–12048.

29 K. Kohse-Höinghaus, B. Atakan, A. Lamprecht, G. González Alatorre, M. Kamphus, T. Kasper and N. Liu, Contributions to the investigation of reaction pathways in fuel-rich flames, *Phys. Chem. Chem. Phys.*, 2002, **4**, 2056–2062.

30 A. R. Brown, J. T. Brice, P. R. Franke and G. E. Douberly, Infrared spectrum of fulvenallene and fulvenallenyl in helium droplets, *J. Phys. Chem. A*, 2019, **123**, 3782–3792.

31 M. Steinbauer, P. Hemberger, I. Fischer and A. Bodi, Photoionization of C_7H_6 and C_7H_5: observation of the fulvenallenyl radical, *Chemphyschem*, 2011, **12**, 1795–1797.

32 D. Polino and C. Cavallotti, Fulvenallene decomposition kinetics, *J. Phys. Chem. A*, 2011, **115**, 10281–10289.

33 G. da Silva and A. J. Trevitt, Chemically activated reactions on the C_7H_5 energy surface: propargyl + diacetylene, i-C_5H_3 + acetylene, and n-C_5H_3 + acetylene, *Phys. Chem. Chem. Phys.*, 2011, **13**, 8940–8952.

34 F. Hirsch, I. Fischer, S. Bakels and A. M. Rijs, Gas-phase infrared spectra of the C_7H_5 radical and its bimolecular reaction products, *J. Phys. Chem. A*, 2022, **126**, 2532–2540.

35 W. Li, J. Yang, L. Zhao, D. Couch, M. S. Marchi, N. Hansen, A. N. Morozov, A. M. Mebel and R. I. Kaiser, Gas-phase preparation of azulene ($C_{10}H_8$) and naphthalene ($C_{10}H_8$) via the reaction of the resonantly stabilized fulvenallenyl and propargyl radicals, *Chem. Sci.*, 2023, **14**, 9795–9805.

36 S. Iglesias-Groth, A. Manchado, R. Rebolo, J. I. González Hernández, D. A. García-Hernández and D. L. Lambert, A search for interstellar anthracene towards the Perseus anomalous microwave emission region, *Mon. Not. R. Astron. Soc.: Lett.*, 2010, **407**, 2157–2165.

37 R. Gredel, Y. Carpentier, G. Rouillé, M. Steglich, F. Huisken and T. Henning, Abundances of PAHs in the ISM: confronting observations with experimental results, *Astron. Astrophys.*, 2011, **530**, A26.

38 L. Gavilan Marin, S. Bejaoui, M. Haggmark, N. Svadlenak, M. de Vries, E. Sciamma-O'Brien and F. Salama, Low-temperature formation of carbonaceous dust grains from PAHs, *Astrophys. J.*, 2020, **889**, 101–119.

39 J. J. Madison and R. M. Roberts, Pyrolysis of aromatics and related heterocyclics, *Ind. Eng. Chem.*, 1958, **50**, 237–250.

40 J. DeCoster, A. Ergut, Y. A. Levendis, H. Richter, J. B. Howard and J. B. Carlson, PAH emissions from high-temperature oxidation of vaporized anthracene, *Proc. Combust. Inst.*, 2007, **31**, 491–499.

41 G. M. Badger, J. K. Donnelly and T. M. Spotswood, The formation of aromatic hydrocarbons at high temperatures. XXIII. The pyrolysis of anthracene, *Aust. J. Chem.*, 1964, **17**, 1147–1156.

42 C. R. Kinney and E. DelBel, Pyrolytic behavior of unsubstituted aromatic hydrocarbons, *Ind. Eng. Chem.*, 1954, **46**, 549–556.

43 M. Liu, Y. Cui, Y. Duan, J. Zhong, W. Sun, M. Wang, S. Liu and Q. Li, Synthesis of metabolites of polycyclic aromatic hydrocarbons, *Mini-Rev. Org. Chem.*, 2010, **7**, 134–144.

44 T. Kaneko, E. Ota, M. Kanazawa and S. Otani, Synthesis and properties of polycondensate of fused polynuclear aromatic (COPNA) resin using anthracene and phenanthrene as raw materials, *Jpn. J. Ophthalmol.*, 1987, **1987**, 1047–1053.

45 H. Bouas-Laurent, A. Castellan and J. P. Desvergne, From anthracene photodimerization to jaw photochromic materials and photocrowns, *Pure Appl. Chem.*, 2009, **52**, 2633–2648.

46 M. Velinova, V. Georgiev, T. Todorova, G. Madjarova, A. Ivanova and A. Tadjer, Boron–nitrogen- and boron-substituted anthracenes and -phenanthrenes as models for doped carbon-based materials, *J. Mol. Struct.*, 2010, **955**, 97–108.

47 Y. Morita, S. Suzuki, K. Sato and T. Takui, Synthetic organic spin chemistry for structurally well-defined open-shell graphene fragments, *Nat. Chem.*, 2011, **3**, 197–204.

48 J. Trotter, The crystal and molecular structure of phenanthrene, *Acta Crystallogr.*, 1963, **16**, 605–608.

49 H. Takeuchi, Structures, stability, and growth sequence patterns of small homoclusters of naphthalene, anthracene, phenanthrene, phenalene, naphthacene, and pyrene, *Comput. Theor. Chem.*, 2013, **1021**, 84–90.

50 S. A. Kudchadker, A. P. Kudchadker and B. J. Zwolinski, Chemical thermodynamic properties of anthracene and phenanthrene, *J. Chem. Thermodyn.*, 1979, **11**, 1051–1059.

51 J. K. Bin and J. I. Hong, Efficient blue organic light-emitting diode using anthracene-derived emitters based on polycyclic aromatic hydrocarbons, *Org. Electron.*, 2011, **12**, 802–808.

52 W. Wang, S. Simonich, B. Giri, Y. Chang, Y. Zhang, Y. Jia, S. Tao, R. Wang, B. Wang, W. Li, J. Cao and X. Lu, Atmospheric concentrations and air-soil gas exchange of polycyclic aromatic hydrocarbons (PAHs) in remote, rural village and urban areas of Beijing-Tianjin region, North China, *Sci. Total Environ.*, 2011, **409**, 2942–2950.

53 C. Zhou, X. Zhu, Z. Wang, X. Ma, J. Chen, Y. Ni, W. Wang, J. Mu and X. Li, Gas-particle partitioning of PAHs in the urban air of Dalian, China: measurements and assessments, *Polycyclic Aromat. Compd.*, 2013, **33**, 31–51.

54 R. I. Kaiser, L. Zhao, W. Lu, M. Ahmed, V. S. Krasnoukhov, V. N. Azyazov and A. M. Mebel, Unconventional excited-state dynamics in the concerted benzyl (C_7H_7) radical self-reaction to anthracene ($C_{14}H_{10}$), *Nat. Commun.*, 2022, **13**, 786.

55 T. Lu and F. Chen, Multiwfn: a multifunctional wavefunction analyzer, *J. Comput. Chem.*, 2012, **33**, 580–592.

56 V. V. Kislov and A. M. Mebel, The formation of naphthalene, azulene, and fulvalene from cyclic C_5 species in combustion: an ab initio/RRKM study of 9-H-fulvalenyl (C_5H_5-C_5H_4) radical rearrangements, *J. Phys. Chem. A*, 2007, **111**, 9532–9543.

57 C. He, R. I. Kaiser, W. Lu, M. Ahmed, Y. Reyes, S. F. Wnuk and A. M. Mebel, Exotic reaction dynamics in the gas-phase preparation of anthracene ($C_{14}H_{10}$) via spiroaromatic radical transients in the indenyl-cyclopentadienyl radical-radical reaction, *J. Am. Chem. Soc.*, 2023, **145**, 3084–3091.

58 A. M. Mebel and V. V. Kislov, Can the $C_5H_5 + C_5H_5 \rightarrow C_{10}H_{10} \rightarrow C_{10}H_9 + H/C_{10}H_8 + H_2$ reaction produce naphthalene? An ab initio/RRKM study, *J. Phys. Chem. A*, 2009, **113**, 9825–9833.

59 G. da Silva, A. J. Trevitt, M. Steinbauer and P. Hemberger, Pyrolysis of fulvenallene (C_7H_6) and fulvenallenyl (C_7H_5): theoretical kinetics and experimental product detection, *Chem. Phys. Lett.*, 2011, **517**, 144–148.

60 A. W. Jasper and N. Hansen, Hydrogen-assisted isomerizations of fulvene to benzene and of larger cyclic aromatic hydrocarbons, *Proc. Combust. Inst.*, 2013, **34**, 279–287.

61 D. E. Couch, A. W. Jasper, G. Kukkadapu, M. M. San Marchi, A. J. Zhang, C. A. Taatjes and N. Hansen, Molecular weight growth by the phenyl + cyclopentadienyl reaction: well-skipping, ring-opening, and dissociation, *Combust. Flame*, 2022, **257**, 112439.

62 W. Li, L. Zhao and R. I. Kaiser, A unified reaction network on the formation of five-membered ringed polycyclic aromatic hydrocarbons (PAHs) and their role in ring expansion processes through radical-radical reactions, *Phys. Chem. Chem. Phys.*, 2023, **25**, 4141–4150.

63 V. S. Krasnoukhov, M. V. Zagidullin, I. P. Zavershinskiy and A. M. Mebel, Formation of phenanthrene via recombination of indenyl and cyclopentadienyl radicals: a theoretical study, *J. Phys. Chem. A*, 2020, **124**, 9933–9941.

64 A. M. Mebel, W. Li, L. Pratali Maffei, C. Cavallotti, A. N. Morozov, C.-Y. Wang, J.-Z. Yang, L. Zhao and R. I. Kaiser, Fulvenallenyl radical ($C_7H_5^{\bullet}$)-mediated gas-phase synthesis of bicyclic aromatic $C_{10}H_8$ isomers: can fulvenallenyl efficiently react with closed-shell hydrocarbons?, *J. Phys. Chem. A*, 2024, **128**, 5707–5720.

65 M. I. Christie, The recombination of halogen atoms, *J. Am. Chem. Soc.*, 1962, **84**, 4066–4070.

66 M. López-Puertas, B. M. Dinelli, A. Adriani, B. Funke, M. García-Comas, M. L. Moriconi, E. D'Aversa, C. Boersma and L. J. Allamandola, Analysis of VIMS near-IR spectra in Titan's upper atmosphere: evidence for heavy and abundant aromatic hydrocarbons, *European Planetary Science Congress*, 2013, **8**, 274–275.

67 L. Zhao, R. I. Kaiser, B. Xu, U. Ablikim, M. Ahmed, M. M. Evseev, E. K. Bashkirov, V. N. Azyazov and A. M. Mebel, Low-temperature formation of polycyclic aromatic hydrocarbons in Titan's atmosphere, *Nature Astronomy*, 2018, **2**, 973–979.

68 J. C. Loison, M. Dobrijevic and K. M. Hickson, The photochemical production of aromatics in the atmosphere of Titan, *Icarus*, 2019, **329**, 55–71.

69 W. Yuan, Y. Li, P. Dagaut, J. Yang and F. Qi, Investigation on the pyrolysis and oxidation of toluene over a wide range conditions. I. Flow reactor pyrolysis and jet stirred reactor oxidation, *Combust. Flame*, 2015, **162**, 3–21.

70 G. T. Buckingham, T. K. Ormond, J. P. Porterfield, P. Hemberger, O. Kostko, M. Ahmed, D. J. Robichaud, M. R. Nimlos, J. W. Daily and G. B. Ellison, The thermal decomposition of the benzyl radical in a heated micro-reactor. I. Experimental findings, *J. Chem. Phys.*, 2015, **142**, 044307.

71 C. He, A. M. Thomas, G. R. Galimova, A. N. Morozov, A. M. Mebel and R. I. Kaiser, Gas-phase formation of fulvenallene (C_7H_6) via the Jahn-Teller distorted tropyl (C_7H_7) radical intermediate under single-collision conditions, *J. Am. Chem. Soc.*, 2020, **142**, 3205–3213.

72 J. Bouwman, M. N. McCabe, C. N. Shingledecker, J. Wandishin, V. Jarvis, E. Reusch, P. Hemberger and A. Bodi, Five-membered ring compounds from the ortho-benzyne + methyl radical reaction under interstellar conditions, *Nature Astronomy*, 2023, **7**, 423–430.